Rolling Element Fault Diagnosis Based on VMD and Sensitivity MCKD

HONGJIANG CUI[1], YING GUAN[1], AND HUAYUE CHEN[2]
[1]College of Locomotive and Rolling Stock Engineering, Dalian Jiaotong University, Dalian 116028, China
[2]School of Computer Science, China West Normal University, Nanchong 637002, China

Corresponding author: Ying Guan (irisguanying@163.com)

ABSTRACT In order to improve the diagnosis accuracy and solve the weak fault signal of rolling element of rolling bearings due to long transmission path, a novel fault diagnosis method based on variational mode decomposition (VMD) and maximum correlation kurtosis deconvolution (MCKD), namely VMD-MCKD-FD is proposed for rolling elements of rolling bearings in this paper. In the proposed VMD-MCKD-FD, the vibration signal of rolling element of rolling bearings is decomposed into a series of Intrinsic Mode Functions (IMFs) by using VMD method. Then the number of modes with outstanding fault information is determined by Kurtosis criterion in order to calculate the deconvolution period T. The periodic fault component of reconstructed signal is enhanced by using sensitivity MCKD method. Finally, the power spectrum of the reconstructed signal is analyzed in detail in order to obtain the fault frequency and diagnose the rolling element fault of rolling bearings. The simulation signal and actual vibration signal are selected to verify the effectiveness of the VMD-MCKD-FD method. The experimental results show that the VMD-MCKD-FD method can effectively diagnose the rolling element fault of rolling bearings and obtain better fault accuracy.

INDEX TERMS Fault diagnosis, rolling element, signal decomposition, VMD, MCKD, feature extraction.

I. INTRODUCTION

As one of the core components in industrial production, rolling bearings are widely applied in various rotating machinery. Therefore, it is very necessary to accurately diagnose faults of rolling bearings [1]–[3]. Rolling bearing faults mainly occur in the inner race, outer race and rolling element [4]–[7]. In recent years, most of researches focus on the fault of the rolling bearing outer race and inner race, and these methods are very effective, while the faults of the rolling elements are less studied [8]–[13]. Because the rolling elements are located inside the rolling bearings, the fault signal of the rolling elements is easily interfered by the external environment during the transmission [14]–[18]. Therefore, it is necessary to diagnose the faults of rolling elements of rolling bearings.

To effectively extract fault features from vibration signal of rolling bearings, a lot of experts have proposed effective feature extraction methods, such as wavelet

The associate editor coordinating the review of this manuscript and approving it for publication was Dazhong Ma.

transform (WT) [19], Hilbert-Huang transform [20], empirical mode decomposition (EMD) [21], Ensemble EMD (EEMD) [22], and so on [23]–[28]. Although these methods can better extract fault features, they still exist deficiencies in processing vibration signals. The WT is not an adaptive signal analysis method, and it requires to choose wavelet basis function in advance [29]–[33]. The EMD is limited due to mode mixing. Although the EEMD can solve the mode mixing problem, the increase of iterations results in the increase of computation time [34]–[39]. Zhao and Ye [40] gave the concept of singular value decomposition packet to realize signal decomposition. Guo and Deng [41] proposed an improved EMD to effectively extract fault features of inner and outer race. Hou *et al.* [42] proposed a weak fault feature extraction method based on optimized sparse coding and approximate SVD. Liu *et al.* [43] proposed a feature extraction method using EEMD and curve code. Zheng *et al.* [44] proposed a fault diagnosis method based on feature extraction and bag-of-words. Kuncan *et al.* [45] proposed a one-dimensional ternary pattern method to extract the features of rolling bearings.

Li et al. [46] proposed a new feature extraction method using EWT and improved MCKD with grid search. Zhou et al. [47] proposed a hybrid fault diagnosis method based on parameter-adaptive VMD and multi-point optimal minimum entropy deconvolution. Li et al. [48] proposed a double-feedback cascaded monostable stochastic resonance system by signal-to-noise ratio. Mahgoun et al. [49] proposed a gear fault detection method using VMD. From these methods, it can see that the VMD can extract fault features from vibration signals. However, there are still residual noise components in IMFs under strong noise interference. The MCKD method is a new deconvolution method, which highlights the periodic impact of fault signals by designing the optimal FIR filter [50]. It is helpful to the fault diagnosis of rolling bearings. Ren et al. [51] combined MCKD with EEMD to diagnose faults. Zhao and Li [52] proposed a new method based on combining MCKD with EMD to diagnose the weak faults. But these methods did not improve the weaknesses of the EMD and EEMD. Wang et al. [53] proposed a new fault diagnosis method for rolling bearings. In addition, some latest fault diagnosis methods are proposed for or rolling bearings. Wang and He [54] proposed a wavelet packet envelope manifold (WPEM) approach to extract the intrinsic envelope structure for well identification of the specific characteristic frequency. Sun et al. [55] proposed a novel intelligent diagnosis method based on the idea of compressed sensing and deep learning for fault identification of rotating machines. Udmale and Singh [56] proposed a novel intelligent diagnosis method using spectral kurtosis and extreme learning machine for fault classification of rotating machines. Hu et al. [57] proposed a new and adaptive spectral kurtosis method for the bearing fault detection. Li et al. [58] proposed an enhanced FBE (EFBE) adopting WPT as the filter of FBE to overcome the shortcomings of the original FBE. Chen et al. [59] proposed a novel method to find formal languages, written with signal spectral logic (SSL), to describe the fault behaviors among frequency domain for fault diagnosis. The other some methods are also proposed to realize the fault diagnosis of rolling bearings [60]–[62].

To sum up, some experts and scholars have proposed EMD, EEMD, VMD, SVD, MCKD, and so on in order to realize the signal analysis, fault feature extraction and fault diagnosis. These methods can better obtain processing results. But these methods have many deficiencies in analyzing signal, extracting fault features and diagnosing faults for rolling elements of rolling bearings, such as the over decomposition of VMD by improper selection of k, modal aliasing of EMD, presetting parameters of MCKD and so on. In addition, it is very difficult to realize rolling element fault feature extraction and fault diagnosis due to weak fault signal of long transmission path by using the traditional methods. Therefore, in order to solve the weak fault signal of rolling elements of rolling bearings due to the long transmission path and improve the diagnosis accuracy for rolling elements of rolling bearings, the advantages of VMD and MCKD are fully integrated to propose a novel rolling element fault diagnosis method

to obtain better performance in extracting fault features for rolling elements of rolling bearings in this paper. Firstly, the vibration signal is decomposed into some IMFs by using VMD with the robustness. The number of modes with outstanding fault information is determined by Kurtosis criterion in order to calculate the deconvolution period T and IMFs with more fault information are chosen to reconstruct the vibration signal. Then the MCKD with sensitivity is used to enhance the periodic fault component of reconstructed signal. The power spectrum of the reconstructed signal is analyzed in detail in order to obtain the fault frequency and diagnose the rolling element faults of rolling bearings. The proposed method doesn't only eliminate the noise interference, but also solves the problem of selecting k of the VMD. It takes on better effect in extracting weak fault features.

The innovations and main contributions of this paper are described as follows.

- A novel rolling element fault diagnosis method based on combining VMD with MCKD is proposed.
- The VMD with the robustness used to decompose fault vibration signal of rolling element into a series of IMFs.
- The number of modes with outstanding fault information is determined by Kurtosis criterion in order to calculate the deconvolution period T.
- The MCKD with the sensitivity is applied to enhance the periodic fault component of the reconstructed signal.

II. BASIC METHODS
A. KURTOSIS CRITERION
Kurtosis is a dimensionless parameter that describes the sharpness of the waveform and reflects the distribution characteristic of the vibration signal. The expression of kurtosis is described as follow.

$$kur = \frac{E(x - \mu)^4}{\sigma^4} \tag{1}$$

where, μ is the mean of x, x is vibration signal, σ is the standard deviation of x.

The vibration signal is normally distributed, so its kurtosis is about 3. But when there are more impulse components in signal, the kurtosis value increases obviously. The fault information of rolling bearings is often included in these signals with more impulse components. The signal with higher kurtosis has more obvious impulse components and easier to extract fault information.

B. VMD
The VMD is an adaptive signal decomposition method, which decomposes the signal into a series of IMFs according to different center frequencies. The decomposition process is mainly divided into the construction and variational solution.

In the VMD, each IMF is regarded as an AM-FM signal with limited bandwidth, which is described as follow.

$$u_k(t) = A_k(t) \cos(\phi_k(t)) \tag{2}$$

where, $A_k(t)$ is instantaneous amplitude, $\omega_k(t)$ is the instantaneous power of the signal, $\omega_k(t) = d\phi_k(t)/dt$.

The variation problem is to decompose the input signal f into k IMFs, and each IMF signal is analyzed by Hilbert transform, then mix it by means of the estimated center frequency $e^{-j\omega_k t}$. The sum of components is equal to the input signal under the constraint, so the variational problems is described as follow.

$$\begin{cases} min\left\{ \sum_k \left\| \partial_t \left[\left(\delta(t) + \frac{j}{\pi t} \right) * u_k(t) \right] e^{-j\omega t} \right\|_2^2 \right\} \\ s.t. \sum_k u_k = f \end{cases} \quad (3)$$

where, $\{u_k\} = \{u_1, u_2, u_3, \cdots u_k\}$ and $\{\omega_k\} = \{\omega_1, \omega_2, \omega_3, \cdots \omega_k\}$ are IMFs and each IMF's central frequencies.

The quadratic penalty operator α is used to ensure the reconstruction accuracy of the signal, and the Lagrange multiplication operator $\lambda(t)$ is used to maintain the constraint strictness.

$$L(\{u_k\}, \{\omega_k\}, \lambda)$$
$$:= \alpha \sum \left\| \partial_t \left[\left(\delta(t) + \frac{j}{\pi t} \right) u_k(t) \right] e^{-j\omega_k t} \right\|_2^2 \hat{u}_k^{n+1}$$
$$+ \left\| f(t) - \sum_k u_k(t)_2^2 + \lambda(t) \right\|, \left\langle f(t) - \sum_k u_k(t) \right\rangle^k \quad (4)$$

The alternate direction method of multipliers is used to alternatively update $\hat{u}_k^{n+1}$, $\hat{\omega}_k^{n+1}$ is used to get the optimal solution, that is the saddle point of the Lagrangian function of Eq. (4). The Fourier transform of $\hat{u}_k^{n+1}$ is the intrinsic $\hat{\lambda}^{n+1}$ mode functions, so that the set of IMFs $\{u_k\}$ and central frequency $\{\omega_k\}$ can be expressed as follows.

$$\hat{u}_k^{n+1}(\omega) = \frac{\hat{f}(\omega) - \sum_{i \neq k} \hat{u}_i(\omega) + \frac{\hat{\lambda}(\omega)}{2}}{1 + 2\alpha(\omega - \omega_k)^2} \quad (5)$$

$$\omega_k^{n+1} = \frac{\int_0^\infty \omega |\hat{u}_k(\omega)|^2 d\omega}{\int_0^\infty |\hat{u}_k(\omega)|^2 d\omega} \quad (6)$$

C. MCKD

In order to restore the collected signal to the original input signal, the MCKD is used to find a finite impulse response filter according to the maximum correlation kurtosis.

$$y(n) = h(n)^* x(n) + e(n) \quad (7)$$

where, $y(n)$ is the collected signal by the sensor, $x(n)$ is the periodic pulse signal, $h(n)$ is attenuation response of the transmission path, $e(n)$ is the noise component.

The kurtosis is affected by a single or partial high-amplitude pulse, so the periodicity and continuity of the faults signal cannot be fully considered. Therefore, the MCKD uses the correlation kurtosis to extract the pulse sequence.

The correlation kurtosis is described as follow.

$$CK_M(T) = max_f \frac{\sum_{n=1}^N \left(\prod_{m=0}^M x_{n-mT} \right)^2}{\left(\sum_{n=1}^N x_n^2 \right)^{M+1}} \quad (8)$$

Matrix form of optimal filter f is obtained as follow.

$$f = \frac{\|x^2\|}{2\|B^2\|} \left(Y_0 Y_0^T \right)^{-1} \sum_{m=0}^M Y_{mT} A_m \quad (9)$$

where, L is the filter length, T is the deconvolution period, and M is the shift-order.

III. DETERMINATION METHOD OF DECONVOLUTION PERIOD

The MCKD has a strong ability to decrease noise and enhance the signal features, but it needs to preset parameters to ensure the effect of signal processing, such as deconvolution period T, and these advantages depend on the correct selection of T. Only by finding a suitable deconvolution period can the periodic impulse component of the fault signal will be highlighted, and fault frequency will be found in the frequency domain. Conversely, if a wrong value of deconvolution period is determined, the fault frequency will be shielded, which cannot be effectively extracted.

The deconvolution period is actual impulse period of the fault in the vibration signal, which can also be understood as the samples of each revolution. Therefore, in actual operation, all samples are used to calculate the deconvolution period. The value of T can be calculated according to the Eq. (10).

$$T = \frac{S}{S_0} = \frac{f_s * t}{f_0 * t} = \frac{f_s}{f_0} \quad (10)$$

where, S is the number of samples, S_0 is the number of fault samples, t is the time of sampling, f_s is the sampling frequency, and f_0 is fault frequency.

IV. A NOVEL FAULT DIAGNOSIS METHOD
A. THE BASIC IDEA

For the problem that the weak fault features of rolling elements are difficult to be extracted, the other methods usually cannot effectively solve. Therefore, a novel rolling element fault diagnosis method based on VMD and MCKD, namely VMD-MCKD-FD is proposed in this paper. The function of the VMD is to decompose the original signal into k IMFs to extract effective information. Because the VMD needs to be preset a suitable value of k to avoid the under-decomposition problem or over-decomposition problem. The selection of k is a difficult problem, but it can be avoided by signal reconstruction. The improper value of k will directly affect the decomposition result of the signal. If the value of k is too small, the similar components are decomposed to the same time scale, which results in mode aliasing. If the value of k is too large, the false components will appear in the decomposition. Therefore, before the VMD is used to decompose the signal, the number of k is preset as a fixed value.

The different value of k ($k = 2,3,4,5,6,7,8$) is set for VMD to verify the influence of different number of modes. The tested results show that it would be best for the value of k = 5. At the same, a large number of literatures about the value of k for VMD are published to address the issue of VMD [63]–[66]. In most of the literatures, the value of k is 5. Therefore, it would be more beneficial to the VMD that the value of k is taken as 5 according to the experiment, some published papers and our experiences. Therefore, the VMD decomposes the signal into 5 IMFs, and 3 IMFs with larger kurtosis are selected for signal reconstruction according to the kurtosis criterion. Kurtosis value is used to evaluate signal pulse. In the bearing fault diagnosis, it is generally used to evaluate the proportion of fault impact component of signal. The kurtosis value is greater, the more fault information is contained in IMF. There are two reasons for selecting three IMFs in here. Firstly, in the process of weak fault diagnosis, due to the interference of noise, the fault information may also appear in the IMF with the second or third largest kurtosis value. Secondly, three IMFs are selected for signal reconstruction in order to avoid the problem of selecting the K value of VMD. Therefore, we choose the 3 IMFs with the highest kurtosis as useful IMFs. Because it is difficult to use the VMD to extract the fault frequency. Therefore, the MCKD is used to further process the signal, and the maximizing correlation kurtosis is applied to enhance the periodic impulse component to achieve the fault frequency extraction of rolling elements for rolling bearings.

B. IMPLEMENTATION STEPS

The flow of VMD-MCKD-FD is shown in FIGURE 1.

The steps of the VMD-MCKD-FD for rolling elements of rolling bearings are described in detail as follows.

Step 1. Firstly, the fault vibration signals are decomposed into k IMFs by using the VMD method.

Step 2. Then some IMFs with larger kurtosis are selected for reconstruction according to the kurtosis criterion.

Step 3. Calculate deconvolution period T.

Step 4. The MCKD is used to process reconstructed signals, the periodic impulse component is enhanced, and the noise interference is reduced.

Step 5. Finally, the power spectral density is calculated from the Hilbert envelope of the obtained signal, and the fault frequency is found by analyzing the power spectrum, so as to diagnose the rolling element faults.

V. SIMULATION RESULTS

In order to verify the validity of the VMD-MCKD-FD for fault diagnosis of rolling elements of rolling bearings, the simulation signals are formed according to the periodic feature faults of rolling elements.

$$x(t) = x_1(t) + x_2(t) + x_3(t) \qquad (11)$$

where, $x_1(t) = 0.7^* \sin(800\pi t)^* \sin(3000\pi t)$, fault signals $x_2(t) = 2A_i^* e^{-350t_1} \sin(8000\pi t)$, and random noise signal $x_3(t)$. A_i is a sequence of random numbers from 0 to 1.
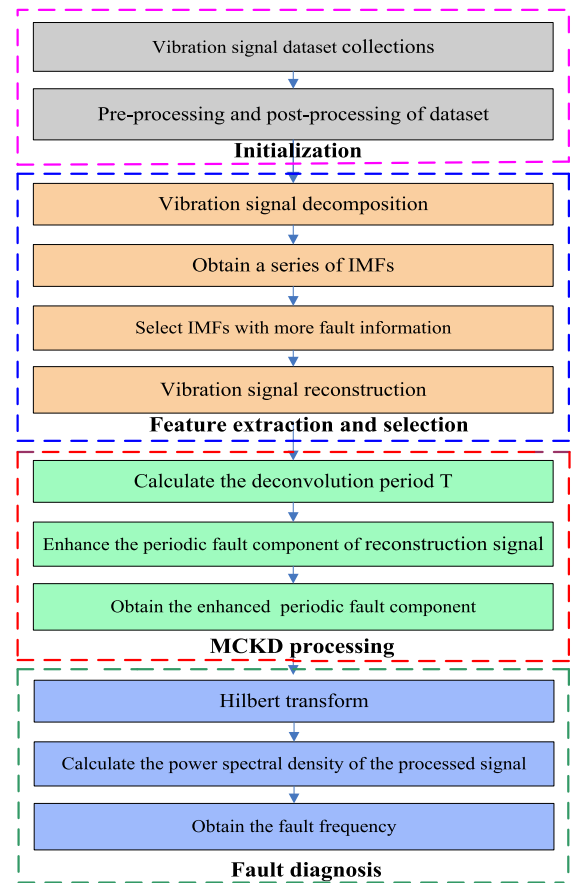

FIGURE 1. The flow of VMD-MCKD-FD for rolling element faults.

Due to the usual slip of rolling elements and cage, the repetition and the experience amplitude are a certain degree of randomness [56], [57], $t_1 = \mathrm{mod}\left(t, \frac{1}{f_0}\right)$, the sampling frequency is 40kHz. After random noise is added, the signal-to-noise ratio (SNR) of the simulation signal is −13.2dB, −8.2 dB and −3.3dB, which simulate the strong noise interference in actual working condition. Finally, the fault frequency f_0 is set as 120Hz. The value of α in VMD is 2000. The time waveform and power spectrum of the simulation signals (−13.2dB, −8.2 dB and −3.3dB) are shown in FIGURE 2, FIGURE 3 and FIGURE 4.

From FIGURE 2 and FIGURE 3, it can be clearly seen that the fault signal is submerged in strong noise (SNR = −13.2 dB and SNR = −8.2 dB), and the valid information of fault frequency or rotating frequency cannot be found. For the simulation signal with less noise (SNR = −3.3 dB), it can be seen that the fault frequency can be found. Therefore, for the simulation signal with strong noise(SNR = −13.2 dB and SNR = −8.2 dB), the VMD method is used to decompose the weak fault signal into 5 IMFs. The time waveforms of 5 IMFs are shown as FIGURE 5 and FIGURE 6.

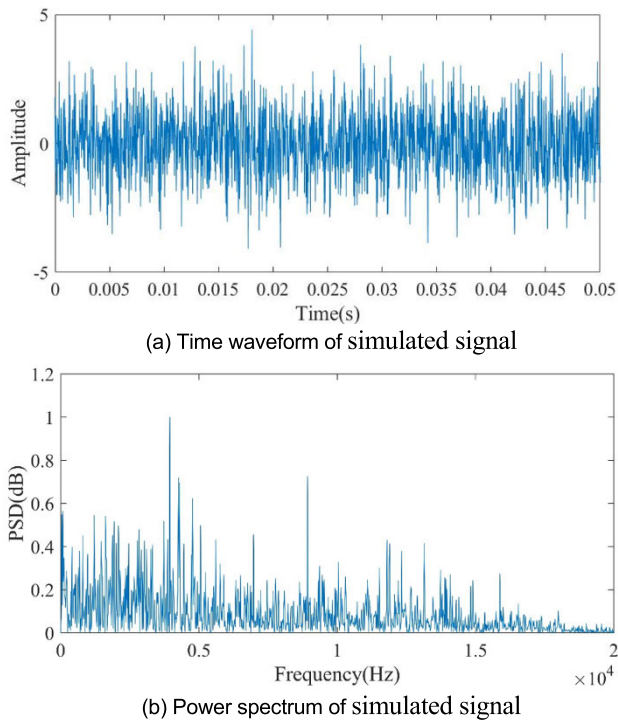From FIGURE 5 and FIGURE 6, the simulation signal is decomposed into 5 IMFs with different frequency

(a) Time waveform of simulated signal

(b) Power spectrum of simulated signal

FIGURE 2. Simulation signal with noise (SNR = −13.2dB).

(a) Time waveform of simulated signal

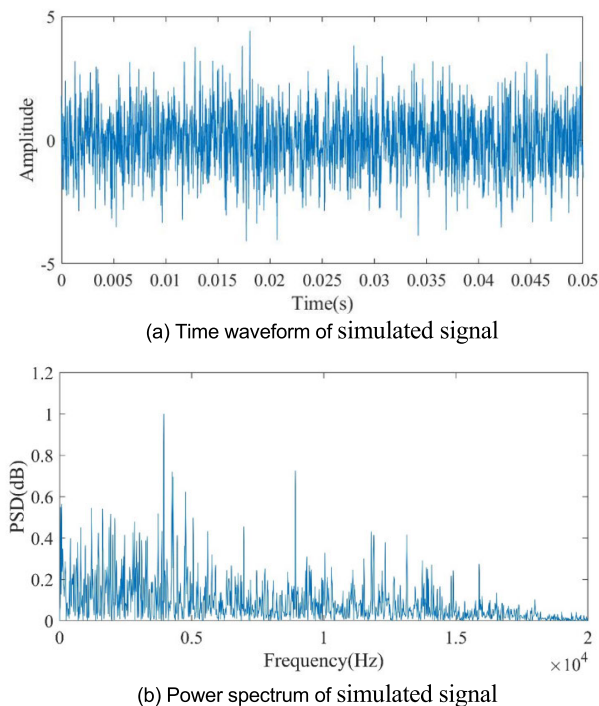(b) Power spectrum of simulated signal

FIGURE 3. Simulation signal with noise (SNR = −8.2dB).

components. Because each IMF contains different frequency components, it is impossible to distinguish which IMF contains more fault information. Therefore, Kurtosis criterion is used to evaluate each IMF, and three frequency components with the largest kurtosis are selected for reconstruction signal.

TABLE 1. Kurtosis index of each IMF of simulated signal.

Index	SNR(dB)	IMF1	IMF2	IMF3	IMF4	IMF5
Kurtosis index	-13.2	3.24	2.69	2.97	2.56	2.85
	-8.2	2.63	3.38	3.15	2.61	2.98

(a) Time waveform of simulated signal

(b) Power spectrum of simulated signal
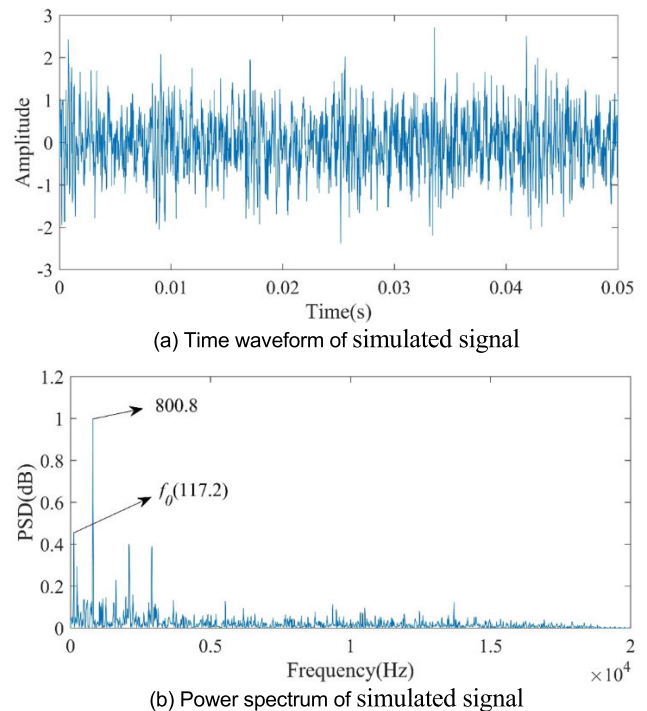
FIGURE 4. Simulation signal with noise (SNR = −3.3dB).

This selection can retain the fault information. The kurtosis indexes of 5 IMFs are shown in TABLE 1.

According to the Kurtosis criterion, IMF1, IMF3 and IMF5 are selected to reconstruct the signal for simulation signal with the noise (SNR = −13.2dB), and IMF2, IMF3 and IMF5 are selected to reconstruct the signal for simulation signal with the noise (SNR-8.3dB). Then the power spectrums of reconstructed signal are shown in FIGURE 7 and FIGURE 8.

Compared with the original signal in FIGURE 2(b) and FIGURE 3(b), the noise interference of reconstructed signal is effectively suppressed in FIGURE 7 and FIGURE 8. However, three most obvious frequency components have no relationship with the fault frequency, which shows that there is still noise interference in the signal. The VMD cannot extract the weak fault feature, so the reconstructed signal needs to be further processed.

According to Eq. (10), the deconvolution period T is calculated to 333. The filter size L is generally in the range of [100,500]. M is generally in the range of [1,7], because the iterative method can reduce the numerical precision if we select a lager M. From experience, L is selected as 300, and M is selected as 5. For the simulation signal with the noise (SNR = −13.2dB), the MCKD is further used to process
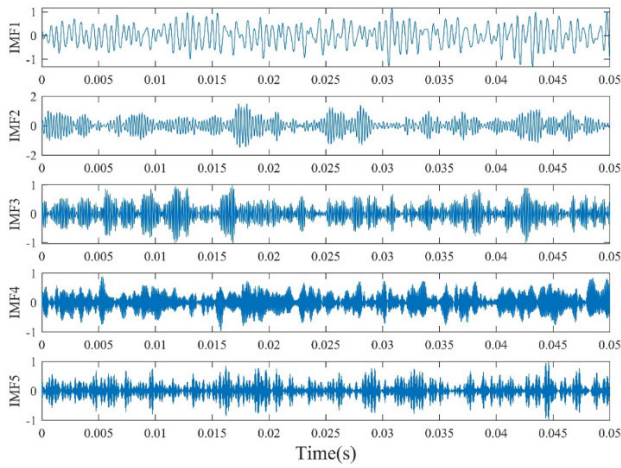
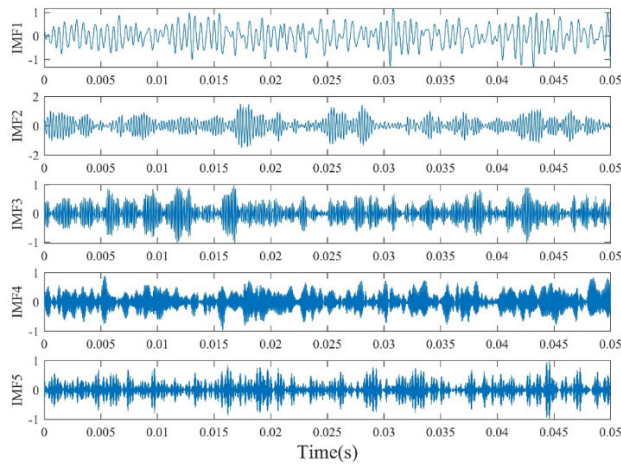**FIGURE 5.** Time waveform of each IMF (SNR = −13.2dB).

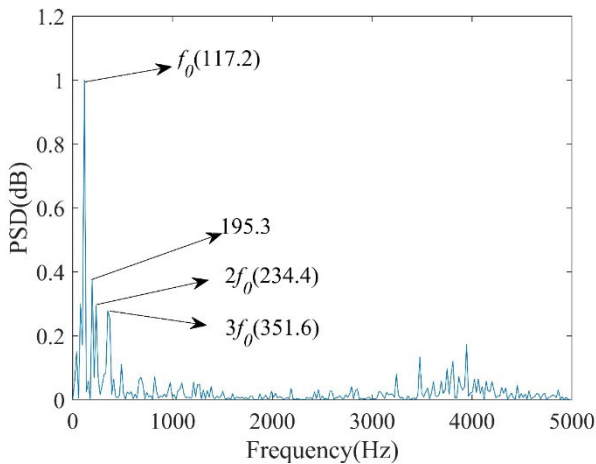**FIGURE 6.** Time waveform of each IMF (SNR = −8.2dB).

FIGURE 7. Power spectrum of simulated signal using VMD (SNR = −13.2dB).
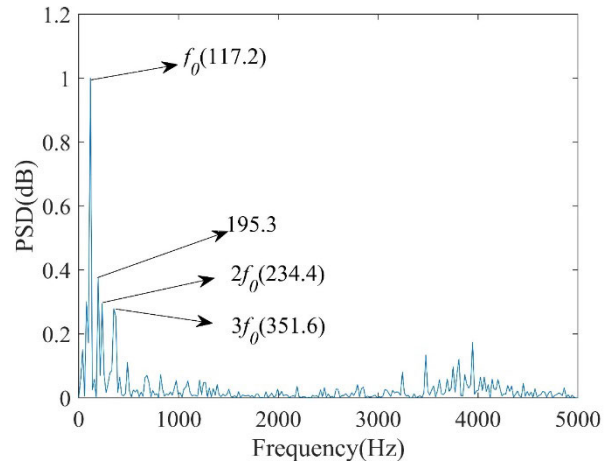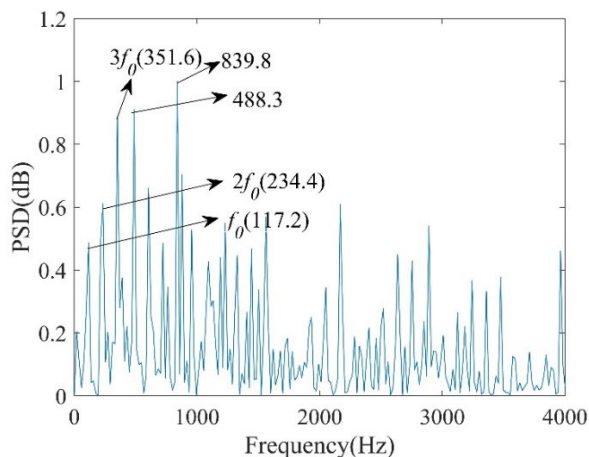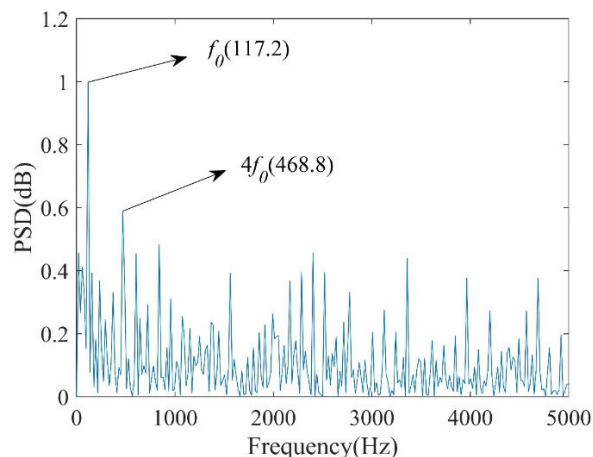

FIGURE 8. Power spectrum of simulated signal using VMD(SNR = −8.2dB).

the EMD and EEMD are selected to decompose the simulation signal, and 3 IMFs with larger kurtosis are selected to reconstruct the signal. These reconstructed signals are processed by using MCKD with same parameters, the power spectrum of processed signals is shown in FIGURE 9(a) and FIGURE 9(b). For the simulation signal with the noise (SNR = −8.2dB), the power spectrums of the simulated signal using EMD-MCKD-FD, EEMD-MCKD-FD and VMD-MCKD-FD are shown in FIGURE 10.
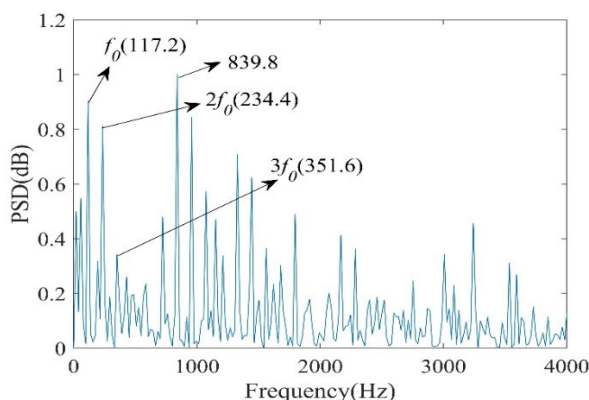
From FIGURE 9(a) and (b), it can be seen that the most obvious frequency component is 839.8Hz. From FIGURE 10 (b), it can be seen that the most obvious frequency component is 957Hz. In FIGURE 9(a), the most obvious frequency component is 839.8Hz, although the fault frequency and its harmonics can be found, but the frequency component with the largest amplitude of them is $3f_0$ (351.6Hz), the fault frequency f_0 (117.2Hz) is not obvious. In FIGURE 9 (b), the frequency component with maximum amplitude is still 839.8Hz, the amplitude of the fault frequency is the second largest. In FIGURE 9(c), the frequency component with the largest amplitude is the fault frequency f_0 (117.2Hz), and the second harmonic is found, the amplitude of other frequency components is relatively small. In FIGURE 10(a), the fault frequency f_0 (117.2Hz) and $4f_0$ (468.8Hz) are found. In FIGURE 10(b), the fault frequency f_0 (117.2Hz) and $4f_0$ (468.8Hz) are found, the other amplitudes of frequency components also exist. In FIGURE 10(c), the fault frequencies f_0 (117.2Hz), $2f_0$ (234.4Hz), $3f_0$ (351.6Hz) and $4f_0$ (468.8Hz) are found, and the other amplitude of frequency components don't exist. Because the collected vibration signal contains some interference signals, which will affect the feature extraction of vibration signal. As a result, the obtained fault frequency has some deviations for dominant frequencies, 117 Hz, 234 Hz, 351Hz and 468Hz. These phenomena show that the VMD has better robustness than EMD and EEMD, and the VMD-MCKD-FD has better performance in extracting the features of weak fault signals.
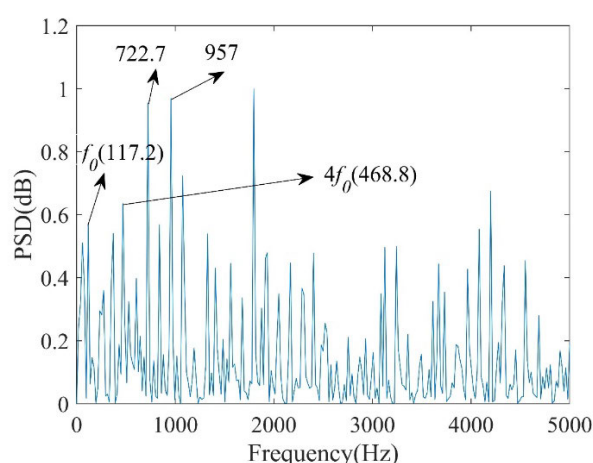
the reconstructed signal, the power spectrum of processed signal is shown in FIGURE 9(c). In order to illustrate the advantages of the VMD to preprocess the vibration signal,
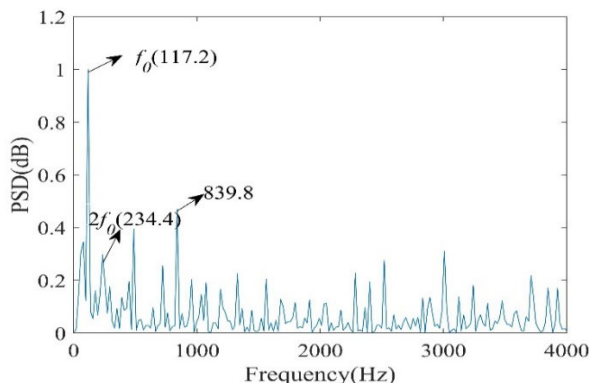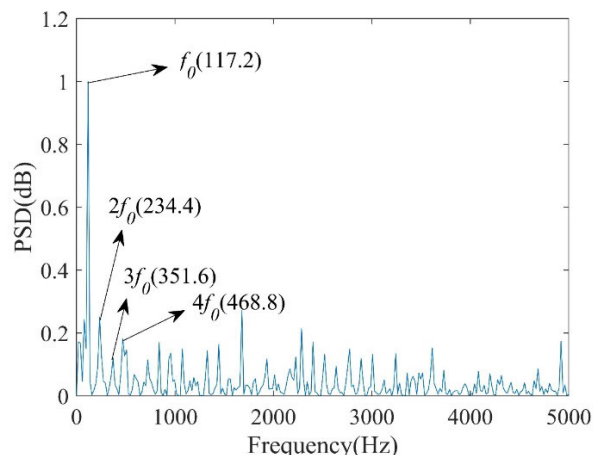
(a) Power spectrum of the simulated signal using EMD-MCKD-FD

(b) Power spectrum of the simulated signal using EEMD-MCKD-FD

(c) Power spectrum of the simulated signal using VMD-MCKD-FD

FIGURE 9. Power spectrum of the simulated signal with noise (SNR = −13.2dB).

(a) Power spectrum of the simulated signal using EMD-MCKD-FD

(b) Power spectrum of the simulated signal using EEMD-MCKD-FD

(c) Power spectrum of the simulated signal using VMD-MCKD-FD

FIGURE 10. Power spectrum of the simulated signal with noise (SNR = −8.2dB).

In order to prove the value of deconvolution period T on the result of feature extraction, the value of T was changed to 250 without changing L and M, and then the reconstructed signal (−13.2dB) is reprocessed. The power spectrum of the simulated signal by using the VMD-MCKD-FD ($T = 250$) is shown in FIGURE11.

It can be seen from FIGURE 11, Three most obvious frequency components in the figure are 17.58Hz, 146.5Hz and

46.88Hz, they are not related to the fault frequency or its harmonics. This phenomenon is due to the fact that the MCKD method can shield the signal component whose impact period is not 250. Therefore, it can be known that the deconvolution
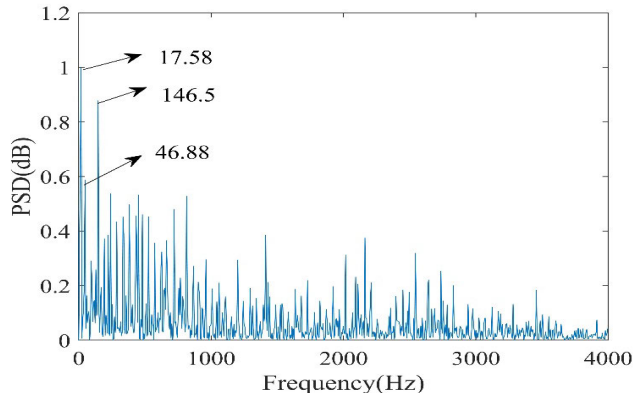
FIGURE 11. Power spectrum of the simulated signal processed by VMD-MCKD ($T = 250$).
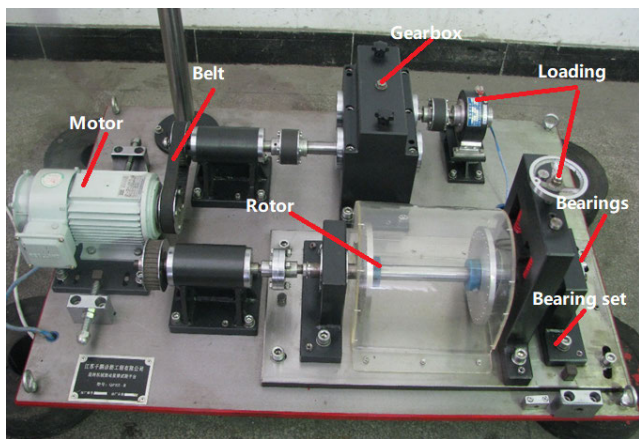

FIGURE 12. The experiment platform of QPZZ-II rotating machinery.

(a) Time waveform of normal signal

(b) Power spectrum of normal signal

FIGURE 13. The normal signal of rolling bearings.

(a) Time waveform of rolling element fault

(b) Power spectrum of rolling element fault

FIGURE 14. The fault signal of rolling elements.

period T should be correctly selected when the MCKD is used to extract fault features, especially for the weak fault feature.
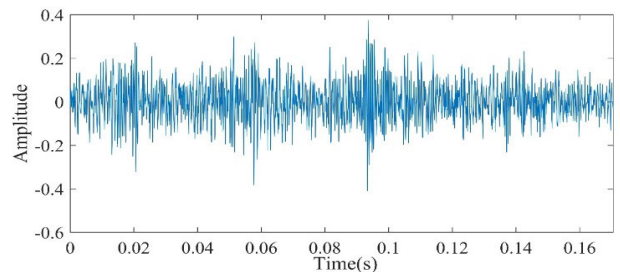
VI. EXPERIMENTAL RESULTS AND ANALYSIS

A. EXPERIMENTAL ENVIRONMENT AND DATA

In order to verify the effectiveness of the VMD-MCKD-FD for the weak fault of rolling elements, the experiment QPZZ-II platform is used to measure the vibration signal of rolling bearings in FIGURE 12. It was measured at a motor speed of 1500r/min and no-load, and the sampling frequency is 12kHz. The experiment used N205 rolling bearings. This bearing contains 13 rolling elements with a diameter of 7.5mm. And the pitch diameter of bearings is 38.5mm. According to the above information, the shaft rotation frequency f_r can be calculated to be about 25Hz, and rolling element fault frequency f_0 is 125.2Hz.
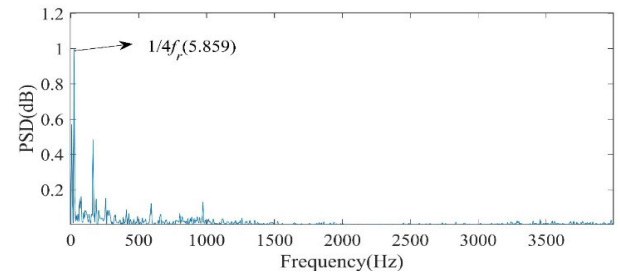
The time waveform and power spectrum of normal signal of rolling bearings are shown in FIGURE 13(a) and FIGURE 13(b).

The time waveform and power spectrum of fault signal of rolling elements are shown in FIGURE 14(a) and (b).

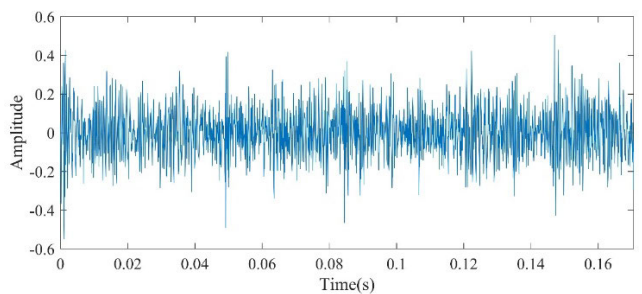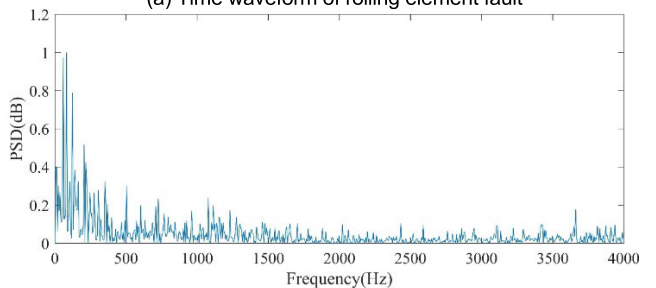From FIGURE 14(a) and FIGURE 14(b), the fault signal of rolling elements of rolling bearings contains strong

noise, the frequency components of the vibration signal are irregularly distributed in the power spectrum, and the invalid information can be extracted. To extract fault features from the weak fault information, the vibration signal needs to be denoised firstly.

B. EXPERIMENTAL RESULT AND ANALYSIS

1) THE RESULTS OF VMD-MCKD-FD

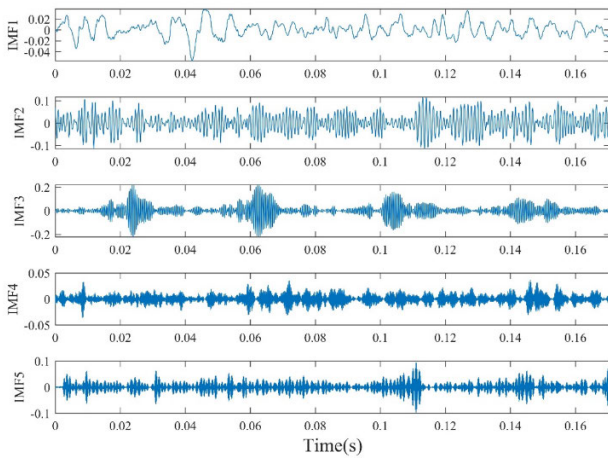The VMD-MCKD-FD method is used to process the normal vibration signal and fault vibration signal of rolling elements

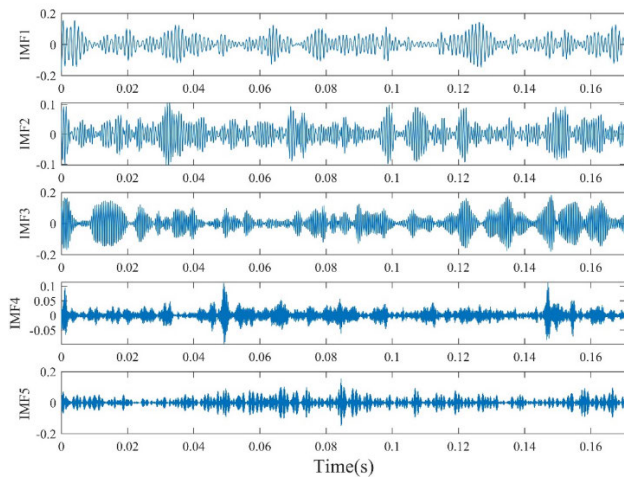**FIGURE 15.** Time waveform of each IMF of normal vibration signal.

FIGURE 16. Time waveform of each IMF of fault vibration signal for rolling elements.

TABLE 2. Kurtosis index of each IMF of normal vibration signal.

	IMF1	IMF2	IMF3	IMF4	IMF5
Kurtosis index	4.08	2.77	6.83	3.46	4.06

TABLE 3. Kurtosis index of each IMF of fault vibration signal of rolling element.

	IMF1	IMF2	IMF3	IMF4	IMF5
Kurtosis index	3.39	3.42	3.60	6.13	3.69
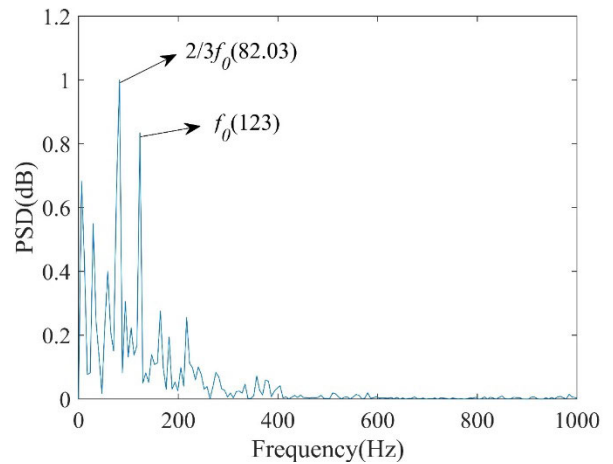
FIGURE 17. Power spectrum of fault vibration signal of rolling elements of rolling bearings using VMD.

of rolling bearings. Firstly, the VMD method is used to decompose the normal vibration signal and fault vibration signal into 5 IMFs. Time waveform of each IMF of the normal vibration signal and fault vibration signal are shown FIGURE 15 and FIGURE 16.

From FIGURE 15 and FIGURE 16, each IMF contains different frequency components. In order to obtain 3 IMFs with more fault information, it is necessary to calculate the Kurtosis value of each IMF. The calculated results are shown in TABLE 2 and TABLE 3.

According to Kurtosis criterion, IMF3, IMF4 and IMF5 are selected to reconstruct the vibration signal. The power spectrum of the reconstructed fault vibration signal of rolling elements of rolling bearings is shown in FIGURE 17.

From FIGURE 17, the fault frequency f_0 (123Hz), and its harmonics $2/3f_0$ (82.03Hz) can be obtained. The frequency component with the largest amplitude is $2/3f_0$, the amplitude of fault frequency is not obvious. This phenomenon shows that the VMD can effectively denoise weak fault signals,

but it is not enough to extract fault frequency. Therefore, the MCKD is used to further process the reconstructed signal.

In order to illustrate the advantages of the VMD-MCKD-FD for processing weak fault vibration signals, the fault vibration signal of rolling elements of rolling bearings is processed by using EMD-MCKD-FD and EEMD-MCKD-FD methods, and the obtained results are compared with the results of the VMD-MCKD-FD. FIGURE18(a) is fault signal power spectrum of the EMD-MCKD-FD, FIGURE18(b) is fault signal power spectrum of the EEMD-MCKD-FD, and FIGURE 18(c) is fault signal power spectrum of the VMD-MCKD-FD. According to Eq. (10), the deconvolution period T is 96. L is selected as 200, and M is selected as 5.

From FIGURE 18(a), $1/2f_r$ (11.72Hz), $5.5f_r$ (128.9Hz) and $4f_0$ (492Hz) can obtained, the frequency component with the largest amplitude is $1/2f_r$. From FIGURE 18(b), the fault frequency and its harmonics can be obtained, but he obtained fault frequency f_0 (123.7Hz) is not very close to the theoretical value(123Hz) and the frequency components with the largest amplitude is also $1/2f_r$ (11.72Hz), and the fault frequency cannot be found. From FIGURE 18(c), the fault frequency f_0 (123 Hz) has the largest amplitude, and its harmonics can also be seen clearly. Therefore, although the
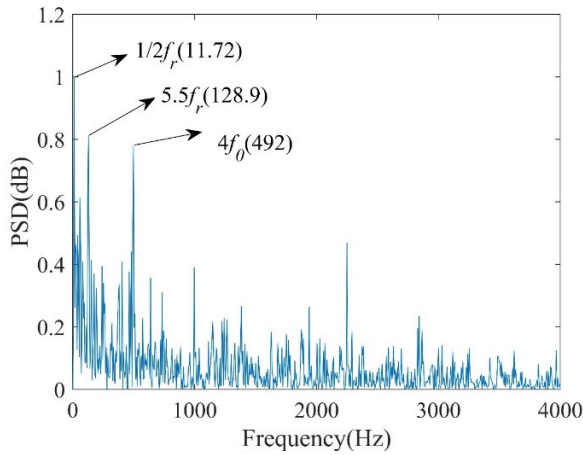
(a) Power spectrum of fault vibration signal using EMD-MCKD-FD

(b) Power spectrum of fault vibration signal using EEMD-MCKD-FD
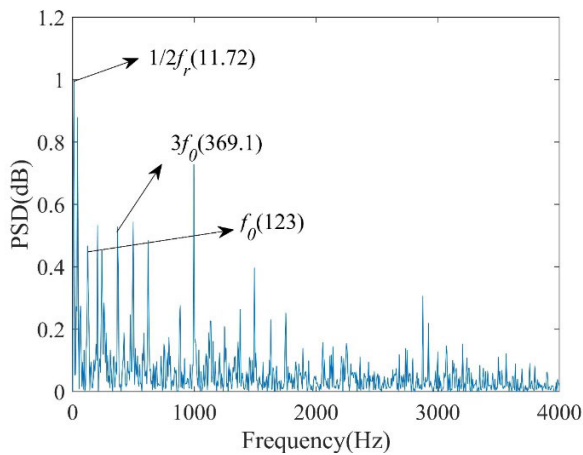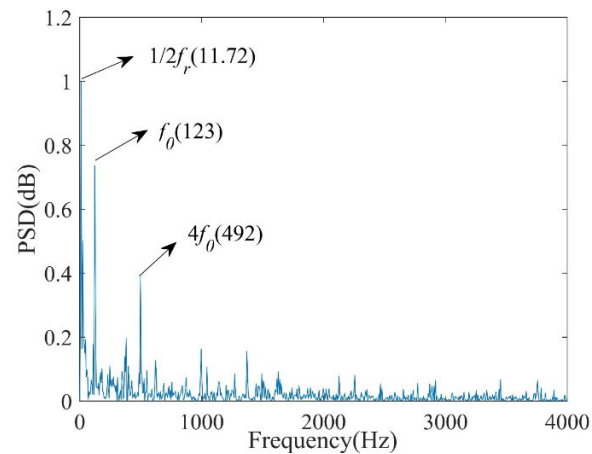

(c) The power spectrum of fault vibration signal using VMD-MCKD-FD

FIGURE 18. Power spectrum of fault vibration signal of rolling elements of rolling bearings using different methods.

FIGURE 19. Power spectrum of fault signal of rolling elements using VMD-MCKD-FD.
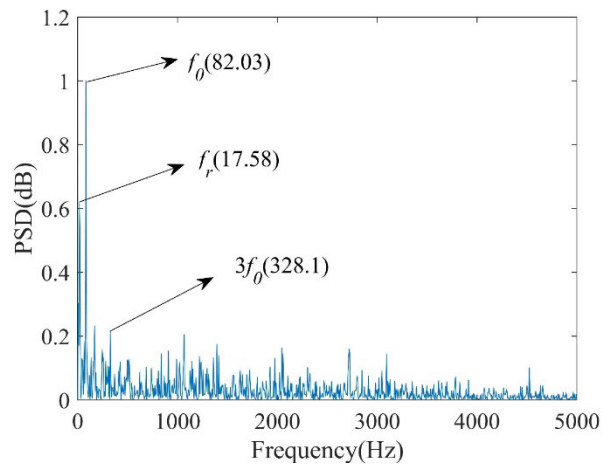
FIGURE 20. Power spectrum of fault signal for rolling elements of the VMD-MCKD-FD.

that the VMD-MCKD-FD takes on better feature extraction performance for the weak faults.

2) THE EFFECT OF DECONVOLUTION PERIOD T ON THE MCKD

To illustrate the effect of the deconvolution period T on the MCKD, the value of T is randomly selected as 150, but the values of L and M have not changed, and then the same method is used to process the reconstructed vibration signal. The power spectrum of reconstructed vibration signal with a wrong deconvolution period is shown in FIGURE 19.

From FIGURE 19, there does not occur fault frequency or harmonic, and the frequency component with the largest amplitude is $2f_r$(46.88Hz). Compared with the processed signal power spectrum by using VMD-MCKD-FD, the incorrect selection of deconvolution period T makes the MCKD unable to find the impact period of the fault signal, the fault information and noise are processed by the filter together, so the fault frequency and its harmonics are obviously shielded. This phenomenon further

EMD-MCKD-FD method and EEMD-MCKD-FD method can also extract the fault frequency and its harmonics, but the amplitude of fault frequency is not obvious in our experiment. In contrast, the VMD-MCKD-FD can more effectively extract the features of weak faults. By comparison, it is found
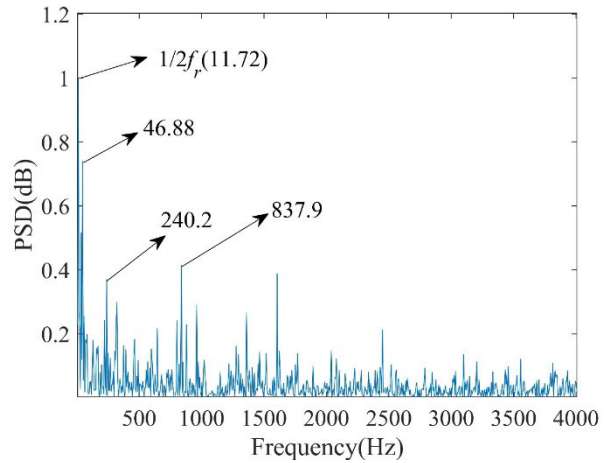
illustrates the importance of a suitable deconvolution period T of the MCKD.

3) THE EFFECT OF VMD-MCKD-FD UNDER DIFFERENT SPEED

In this section, the speed is selected as 1000r/min, and then the experiment is carried out to verify the diagnosis effect of the VMD-MCKD-FD for rolling elements under the different speed. According to the information, the shaft rotation frequency f_r can be calculated to be about 16.7Hz, and the fault frequency f_0 of rolling elements is about 83.5Hz. According to Eq. (10), the deconvolution period T is 144.

From FIGURE 20, the fault frequency f_0 (82.03Hz) and its harmonics $3f_0$ (246.1Hz) can be found. The VMD-MCKD-FD can successfully extract the fault features under different speed.

VII. CONCLUSION

In this paper, a novel rolling element fault diagnosis method (VMD-MCKD-FD) is proposed. In addition, the influence of different selections of the deconvolution period T on MCKD also is analyzed and discussed. The VMD method is mainly used to decompose non-linear and non-stationary vibration signals of rolling elements of rolling bearings. After that, the IMFs with larger kurtosis values are selected for reconstructing the vibration signal. It not only avoids the selection of k in the VMD, but also fully retains the information of fault feature. The MCKD enhances the weak fault feature of rolling elements. In here, the diagnosis results of the EMD-MCKD-FD, EEMD-MCKD-FD and VMD-MCKD-FD with different deconvolution periods T are compared. The simulated and experimental results do not only prove the effectiveness of the VMD-MCKD-FD, but also prove the importance of the deconvolution period T.

The value of T is calculated through theory, but the parameters in real working conditions are slightly different from the theory. Therefore, it should consider how to adaptively select the parameters, and further improve the effect of feature extraction for the weak faults of rolling elements of rolling bearings in the future.

REFERENCES

[1] H. Shao, J. Lin, L. Zhang, D. Galar, and U. Kumar, "A novel approach of multisensory fusion to collaborative fault diagnosis in maintenance," *Inf. Fusion*, vol. 74, pp. 65–76, Oct. 2021.

[2] B. Li, M.-Y. Chow, Y. Tipsuwan, and J. C. Hung, "Neural-network-based motor rolling bearing fault diagnosis," *IEEE Trans. Ind. Electron.*, vol. 47, no. 5, pp. 1060–1069, Oct. 2000.

[3] Y. Fu, Z. Gao, Y. Liu, A. Zhang, and X. Yin, "Actuator and sensor fault classification for wind turbine systems based on fast Fourier transform and uncorrelated multi-linear principal component analysis techniques," *Processes*, vol. 8, no. 9, p. 1066, Sep. 2020.

[4] Y. Song, D. Wu, W. Deng, X.-Z. Gao, T. Li, B. Zhang, and Y. Li, "MPPCEDE: Multi-population parallel co-evolutionary differential evolution for parameter optimization," *Energy Convers. Manage.*, vol. 228, Jan. 2021, Art. no. 113661.

[5] K. Liang, M. Zhao, J. Lin, J. Jiao, and C. Ding, "Maximum average kurtosis deconvolution and its application for the impulsive fault feature enhancement of rotating machinery," *Mech. Syst. Signal Process.*, vol. 149, Feb. 2021, Art. no. 107323.

[6] W. Deng, J. Xu, H. Zhao, and Y. Song, "A novel gate resource allocation method using improved PSO-based QEA," *IEEE Trans. Intell. Transp. Syst.*, early access, Oct. 1, 2020, doi: 10.1109/TITS.2020.3025796.

[7] F. Wang, C. Liu, W. Su, Z. Xue, Q. Han, and H. Li, "Combined failure diagnosis of slewing bearings based on MCKD-CEEMD-ApEn," *Shock Vib.*, vol. 2018, Apr. 2018, Art. no. 6321785.

[8] W. Deng, H. Liu, J. Xu, H. Zhao, and Y. Song, "An improved quantum-inspired differential evolution algorithm for deep belief network," *IEEE Trans. Instrum. Meas.*, vol. 69, no. 10, pp. 7319–7327, Oct. 2020.

[9] D. Huang, S. Li, N. Qin, and Y. Zhang, "Fault diagnosis of high-speed train bogie based on the improved-CEEMDAN and 1-D CNN algorithms," *IEEE Trans. Instrum. Meas.*, vol. 70, 2021, Art. no. 3508811.

[10] X. Li, Y. Yang, H. Shao, X. Zhong, J. Cheng, and J. Cheng, "Symplectic weighted sparse support matrix machine for gear fault diagnosis," *Measurement*, vol. 168, Jan. 2021, Art. no. 108392.

[11] L. Rasolofondraibe, B. Pottier, P. Marconnet, and E. Perrin, "Numerical model of the capacitive probe's capacitance for measuring the external loads transmitted by the bearing's rolling elements of rotating machines," *IEEE Sensors J.*, vol. 13, no. 8, pp. 3067–3072, Aug. 2013.

[12] Y. Ou, S. He, C. Hu, J. Bao, and W. Li, "Research on rolling bearing fault diagnosis using improved majorization-minimization-based total variation and empirical wavelet transform," *Shock Vib.*, vol. 2020, May 2020, Art. no. 3218564.

[13] J. Pan, J. Chen, Y. Zi, Y. Li, and Z. He, "Mono-component feature extraction for mechanical fault diagnosis using modified empirical wavelet transform via data-driven adaptive Fourier spectrum segment," *Mech. Syst. Signal Process.*, vols. 72–73, pp. 160–183, May 2016.

[14] M. Yuan, A. Sadhu, and K. Liu, "Condition assessment of structure with tuned mass damper using empirical wavelet transform," *J. Vib. Control*, vol. 24, no. 20, pp. 4850–4867, Oct. 2018.

[15] Y. Song, D. Wu, A. W. Mohamed, X. Zhou, B. Zhang, and W. Deng, "Enhanced success history adaptive DE for parameter optimization of photovoltaic models," *Complexity*, vol. 2021, Jan. 2021, Art. no. 6660115.

[16] Y. Yang, H. Chen, A. A. Heidari, and A. H. Gandomi, "Hunger games search: Visions, conception, implementation, deep analysis, perspectives, and towards performance shifts," *Expert Syst. Appl.*, vol. 177, Sep. 2021, Art. no. 114864.

[17] J. R. Stack, R. G. Harley, and T. G. Habetler, "An amplitude modulation detector for fault diagnosis in rolling element bearings," *IEEE Trans. Ind. Electron.*, vol. 51, no. 5, pp. 1097–1102, Oct. 2004.

[18] Z. Lei, G. Wen, S. Dong, X. Huang, H. Zhou, Z. Zhang, and X. Chen, "An intelligent fault diagnosis method based on domain adaptation and its application for bearings under polytropic working conditions," *IEEE Trans. Instrum. Meas.*, vol. 70, 2021, Art. no. 3505914.

[19] N. Hazarika, J. Z. Chen, A. C. Tsoi, and A. Sergejew, "Wavelet transform," *Signal Process.*, vol. 59, no. 1, pp. 61–72, 1997.

[20] D. J. Huang, J. P. Zhao, and J. L. Su, "Practical implementation of Hilbert–Huang transform algorithm," *Acta Oceanol. Sinica-English Ed.*, vol. 22, no. 1, pp. 1–14, 2003.

[21] N. E. Huang, Z. Shen, S. R. Long, M. C. Wu, H. H. Shih, Q. Zheng, N.-C. Yen, C. C. Tung, and H. H. Liu, "The empirical mode decomposition and the Hilbert spectrum for nonlinear and non-stationary time series analysis," *Proc. Roy. Soc. London A, Math., Phys. Eng. Sci.*, vol. 454, no. 1971, pp. 903–995, Mar. 1998.

[22] J. Zhang, R. Yan, R. X. Gao, and Z. Feng, "Performance enhancement of ensemble empirical mode decomposition," *Mech. Syst. Signal Process.*, vol. 24, no. 7, pp. 2104–2123, Oct. 2010.

[23] K. Zhong, G. Zhou, W. Deng, Y. Zhou, and Q. Luo, "MOMPA: Multi-objective marine predator algorithm," *Comput. Methods Appl. Mech. Eng.*, vol. 385, Nov. 2021, Art. no. 114029.

[24] S. Lu, P. Zheng, Y. Liu, Z. Cao, H. Yang, and Q. Wang, "Sound-aided vibration weak signal enhancement for bearing fault detection by using adaptive stochastic resonance," *J. Sound Vib.*, vol. 449, pp. 18–29, Jun. 2019.

[25] Y. Peng, Z. Li, K. He, Y. Liu, Q. Li, and L. Liu, "Broadband mode decomposition and its application to the quality evaluation of welding inverter power source signals," *IEEE Trans. Ind. Electron.*, vol. 67, no. 11, pp. 9734–9746, Nov. 2020.

[26] S. Guo, X. Zhang, Y. Du, Y. Zheng, and Z. Cao, "Path planning of coastal ships based on optimized DQN reward function," *J. Mar. Sci. Eng.*, vol. 9, no. 2, p. 210, Feb. 2021.

[27] H. Shao, M. Xia, G. Han, Y. Zhang, and J. Wan, "Intelligent fault diagnosis of rotor-bearing system under varying working conditions with modified transfer convolutional neural network and thermal images," *IEEE Trans. Ind. Informat.*, vol. 17, no. 5, pp. 3488–3496, May 2021.

[28] W. Shan, Z. Qiao, A. A. Heidari, H. Chen, H. Turabieh, and Y. Teng, "Double adaptive weights for stabilization of moth flame optimizer: Balance analysis, engineering cases, and medical diagnosis," *Knowl.-Based Syst.*, vol. 214, Feb. 2021, Art. no. 106728.

[29] D. P. Mandic, N. ur Rehman, Z. Wu, and N. E. Huang, "Empirical mode decomposition-based time-frequency analysis of multivariate signals: The power of adaptive data analysis," *IEEE Signal Process. Mag.*, vol. 30, no. 6, pp. 74–86, Nov. 2013.

[30] J. Hu, H. Chen, A. A. Heidari, M. Wang, X. Zhang, Y. Chen, and Z. Pan, "Orthogonal learning covariance matrix for defects of grey wolf optimizer: Insights, balance, diversity, and feature selection," *Knowl.-Based Syst.*, vol. 213, Feb. 2021, Art. no. 106684.

[31] Z. He, H. Shao, X. Zhang, J. Cheng, and Y. Yang, "Improved deep transfer auto-encoder for fault diagnosis of gearbox under variable working conditions with small training samples," *IEEE Access*, vol. 7, pp. 115368–115377, 2019.

[32] X. Lyu, Z. Hu, H. Zhou, and Q. Wang, "Application of improved MCKD method based on QGA in planetary gear compound fault diagnosis," *Measurement*, vol. 139, pp. 236–248, Jun. 2019.

[33] T. Ma, X. Zhang, H. Jiang, K. Wang, L. Xia, and X. Guan, "Early fault diagnosis of shaft crack based on double optimization maximum correlated kurtosis deconvolution and variational mode decomposition," *IEEE Access*, vol. 9, pp. 14971–14982, 2021.

[34] W. Deng, J. Xu, X.-Z. Gao, and H. Zhao, "An enhanced MSIQDE algorithm with novel multiple strategies for global optimization problems," *IEEE Trans. Syst., Man, Cybern. Syst.*, early access, Nov. 4, 2020, doi: 10.1109/TSMC.2020.3030792.

[35] X. Zhao, X. Zhang, Z. Cai, X. Tian, X. Wang, Y. Huang, H. Chen, and L. Hu, "Chaos enhanced grey wolf optimization wrapped ELM for diagnosis of paraquat-poisoned patients," *Comput. Biol. Chem.*, vol. 78, pp. 481–490, Feb. 2019.

[36] R. B. Randall, J. Antoni, and S. Chobsaard, "The relationship between spectral correlation and envelope analysis in the diagnostics of bearing faults and other cyclostationary machine signals," *Mech. Syst. Signal Process.*, vol. 15, no. 5, pp. 945–962, Sep. 2001.

[37] Y. Wu, C. Zhen, and C. Liu, "Application of variational mode decomposition in wind power fault diagnosis," *J. Mech. Transmiss.*, vol. 39, no. 10, pp. 129–132, Oct. 2015.

[38] Z. Wang, G. He, W. Du, J. Zhou, X. Han, J. Wang, H. He, X. Guo, J. Wang, and Y. Kou, "Application of parameter optimized variational mode decomposition method in fault diagnosis of gearbox," *IEEE Access*, vol. 7, pp. 44871–44882, Apr. 2019.

[39] X. Cai, H. Zhao, S. Shang, Y. Zhou, W. Deng, H. Chen, and W. Deng, "An improved quantum-inspired cooperative co-evolution algorithm with muli-strategy and its application," *Expert Syst. Appl.*, vol. 171, Jun. 2021, Art. no. 114629.

[40] X. Zhao and B. Ye, "Singular value decomposition packet and its application to extraction of weak fault feature," *Mech. Syst. Signal Process.*, vols. 70–71, pp. 73–86, Mar. 2016.

[41] T. Guo and Z. Deng, "An improved EMD method based on the multi-objective optimization and its application to fault feature extraction of rolling bearing," *Appl. Acoust.*, vol. 127, pp. 46–62, Dec. 2017.

[42] F. Hou, J. Chen, and G. Dong, "Weak fault feature extraction of rolling bearings based on globally optimized sparse coding and approximate SVD," *Mech. Syst. Signal Process.*, vol. 111, pp. 234–250, Oct. 2018.

[43] D. Liu, Z. Xiao, X. Hu, C. Zhang, and O. P. Malik, "Feature extraction of rotor fault based on EEMD and curve code," *Measurement*, vol. 135, pp. 712–724, Mar. 2019.

[44] H. Zheng, G. Cheng, Y. Li, and C. Liu, "A new fault diagnosis method for planetary gear based on image feature extraction and bag-of-words model," *Measurement*, vol. 145, pp. 1–13, Oct. 2019.

[45] M. Kuncan, K. Kaplan, M. R. Minaz, Y. Kaya, and H. M. Ertunç, "A novel feature extraction method for bearing fault classification with one dimensional ternary patterns," *ISA Trans.*, vol. 100, pp. 346–357, May 2020.

[46] L. Li, A. Guo, and H. Chen, "Feature extraction based on EWT with scale space threshold and improved MCKD for fault diagnosis," *IEEE Access*, vol. 9, pp. 45407–45417, 2021.

[47] X. Zhou, Y. Li, L. Jiang, and L. Zhou, "Fault feature extraction for rolling bearings based on parameter-adaptive variational mode decomposition and multi-point optimal minimum entropy deconvolution," *Measurement*, vol. 173, Mar. 2021, Art. no. 108469.

[48] J. Li, X. Wang, Z. Li, and Y. Zhang, "Stochastic resonance in cascaded monostable systems with double feedback and its application in rolling bearing fault feature extraction," *Nonlinear Dyn.*, vol. 104, no. 2, pp. 971–988, Apr. 2021, doi: 10.1007/s11071-021-06369-4.

[49] H. Mahgoun, F. Chaari, and A. Felkaoui, "Detection of gear faults using variational mode decomposition (VMD)," *Mech. Ind.*, vol. 17, no. 2, p. 207, Feb. 2016.

[50] G. L. McDonald, Q. Zhao, and M. J. Zuo, "Maximum correlated Kurtosis deconvolution and application on gear tooth chip fault detection," *Mech. Syst. Signal Process.*, vol. 33, pp. 237–255, Nov. 2012.

[51] X. Ren, C. Wang, and Y. Zhang, "Feature extraction of rolling Bearing's weak fault based on MCKD-EEMD," *Machinery Des. Manuf.*, vol. 8, pp. 193–196, Aug. 2016.

[52] H. Zhao and L. Li, "Incipient bearing fault diagnosis based on MCKD-EMD for wind turbine," *Electr. Power Autom. Equip.*, vol. 37, no. 2, pp. 29–36, Feb. 2017.

[53] J. Wang, S. Chen, and C. Zhang, "Application and research of VMD and MCKD in bearing fault diagnosis," *Modular Mach. Tool Autom. Manuf. Technique*, vol. 5, pp. 69–72, May 2017.

[54] J. Wang and Q. He, "Wavelet packet envelope manifold for fault diagnosis of rolling element bearings," *IEEE Trans. Instrum. Meas.*, vol. 65, no. 11, pp. 2515–2526, Nov. 2016.

[55] J. Sun, C. Yan, and J. Wen, "Intelligent bearing fault diagnosis method combining compressed data acquisition and deep learning," *IEEE Trans. Instrum. Meas.*, vol. 67, no. 1, pp. 185–195, Jan. 2018.

[56] S. S. Udmale and S. K. Singh, "Application of spectral kurtosis and improved extreme learning machine for bearing fault classification," *IEEE Trans. Instrum. Meas.*, vol. 68, no. 11, pp. 4222–4233, Nov. 2019.

[57] Y. Hu, W. Bao, X. Tu, F. Li, and K. Li, "An adaptive spectral kurtosis method and its application to fault detection of rolling element bearings," *IEEE Trans. Instrum. Meas.*, vol. 69, no. 3, pp. 739–750, Mar. 2020.

[58] H. Li, T. Liu, X. Wu, and Q. Chen, "Enhanced frequency band entropy method for fault feature extraction of rolling element bearings," *IEEE Trans. Ind. Informat.*, vol. 16, no. 9, pp. 5780–5791, Sep. 2020.

[59] G. Chen, P. Wei, H. Jiang, and M. Liu, "Formal language generation for fault diagnosis with spectral logic via adversarial training," *IEEE Trans. Ind. Informat.*, early access, Nov. 26, 2020, doi: 10.1109/TII.2020.3040743.

[60] H. Zhao, H. Liu, Y. Jin, X. Dang, and W. Deng, "Feature extraction for data-driven remaining useful life prediction of rolling bearings," *IEEE Trans. Instrum. Meas.*, vol. 70, 2021, Art. no. 3511910.

[61] P. Shi, S. An, P. Li, and D. Han, "Signal feature extraction based on cascaded multi-stable stochastic resonance denoising and EMD method," *Measurement*, vol. 90, pp. 318–328, Aug. 2016.

[62] H. Cui, Y. Guan, H. Chen, and W. Deng, "A novel advancing signal processing method based on coupled multi-stable stochastic resonance for fault detection," *Appl. Sci.*, vol. 11, no. 12, p. 5385, Jun. 2021.

[63] W. Deng, S. Shang, X. Cai, H. Zhao, Y. Song, and J. Xu, "An improved differential evolution algorithm and its application in optimization problem," *Soft Comput.*, vol. 25, no. 7, pp. 5277–5298, Apr. 2021.

[64] Q. Xiao, J. Li, and Z. Zeng, "A denoising scheme for DSPI phase based on improved variational mode decomposition," *Mech. Syst. Signal Process.*, vol. 110, pp. 28–41, Sep. 2018.

[65] W. Deng, S. Shang, X. Cai, H. Zhao, Y. Zhou, H. Chen, and W. Deng, "Quantum differential evolution with cooperative coevolution framework and hybrid mutation strategy for large scale optimization," *Knowl.-Based Syst.*, vol. 224, Jul. 2021, Art. no. 107080.

[66] H. Liu, D. Li, Y. Yuan, S. Zhang, H. Zhao, and W. Deng, "Fault diagnosis for a bearing rolling element using improved VMD and HT," *Appl. Sci.*, vol. 9, no. 7, p. 1439, Apr. 2019.